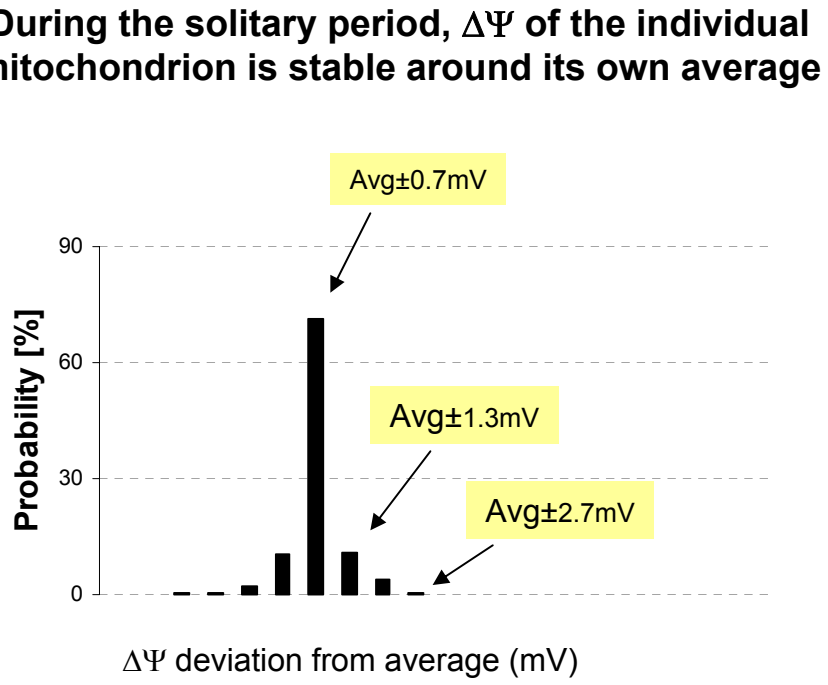

Figure S1: Stability of membrane potential of mitochondria during the solitary period. This histogram reflects cumulative data from 300 minutes of membrane potential tracking of 17 mitochondria from 17 different cells. For each mitochondrion the average membrane potential over time was determined and the probability for deviations from the average is presented. Note that mitochondria reside close to their own average. A deviation of more than 2.7mV is a rare event.

Figure S1

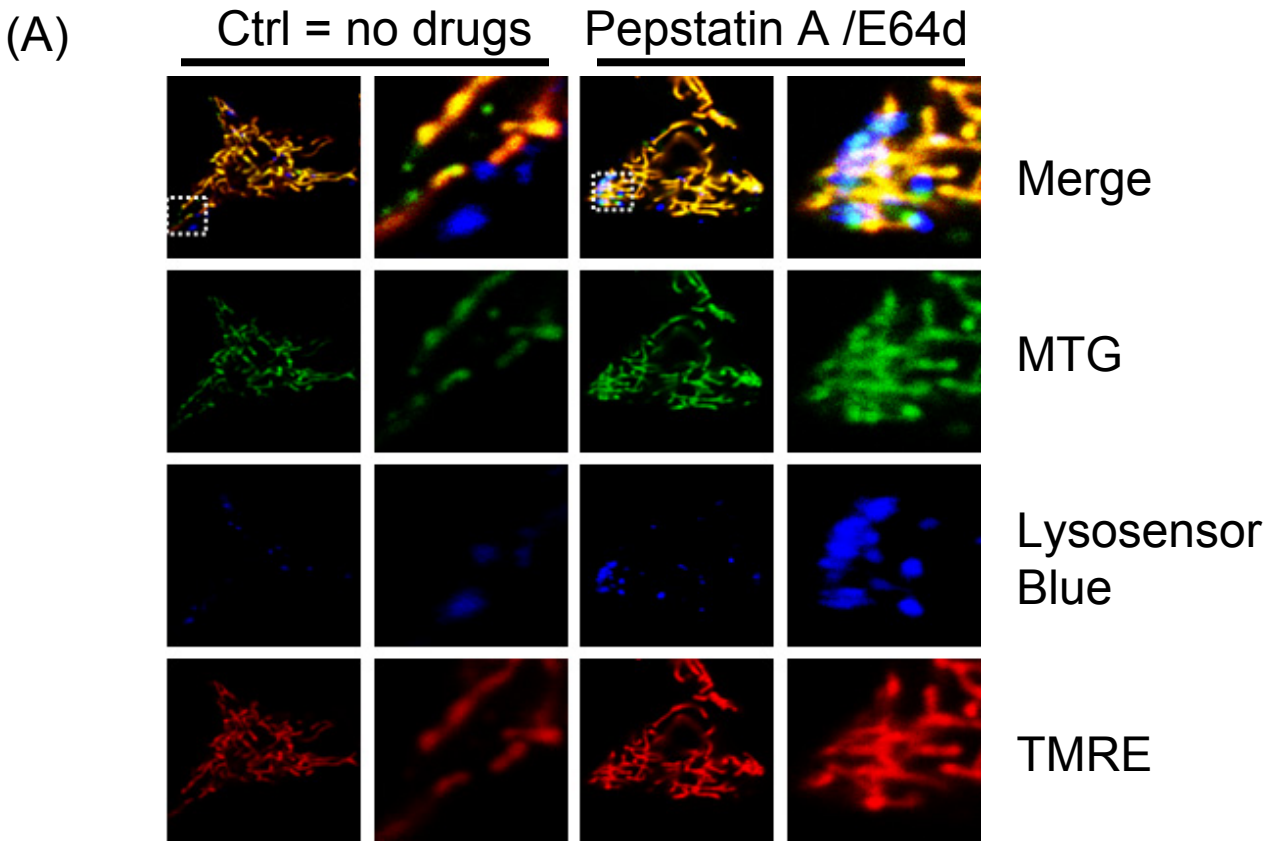

Figure S2: Localization of mitochondria in autophagosomes and autolysosomes is rarely seen under normal conditions. (A) Triple staining with TMRE, MTG and LysoSensor Blue was performed to observe colocalization of autophagolysosomes and depolarized mitochondria. It is evident that in the control conditions (two left columns), depolarized mitochondria are rarely engulfed by lysosomes. However, 30 min incubation with pepstatin A and E64D (two right columns) which inhibit autolysosome formation, led to accumulation of depolarized mitochondria within lysosomes.

Figure S2

(B)

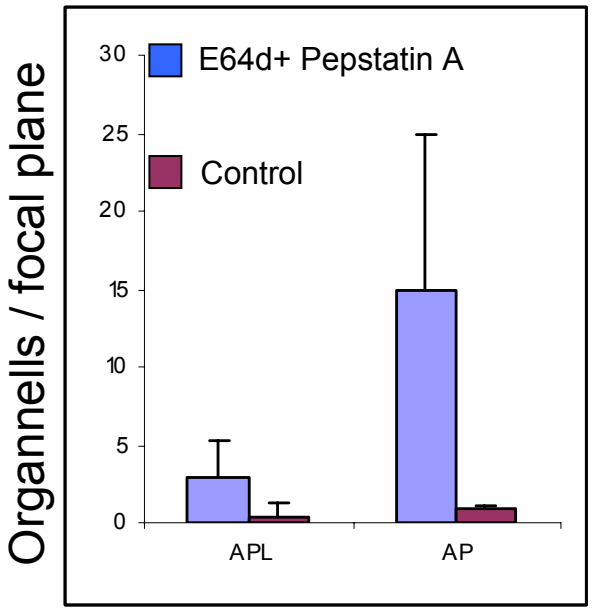

APL= autophagolysosoome (Lysosensor+ mitochondria)
AP=autophagosome (LC-3 +mitochondria)

(C)

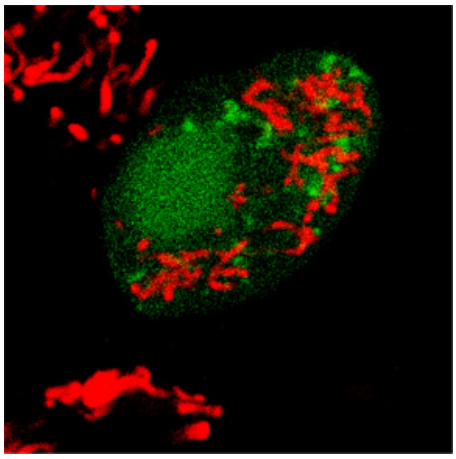

TMRE -red
LC3-GFP -green

Figure S2 continued:
(B) Summary of autophagosomes (AP)-containing mitochondria (colocalization of LC3 and Mitotracker red) and APL with and without pepstatin A (n=6). These results indicate that under control conditions depolarized mitochondria are rarely seen within autophagosomes or autolysosomes and that once the process of autophagy was initiated, it was a rapid process. (C) LC3:GFP and TMRE staining in a living INS1 cell show that polarized mitochondria cannot be seen in APs as identified by LC3:GFP.

Figure S2

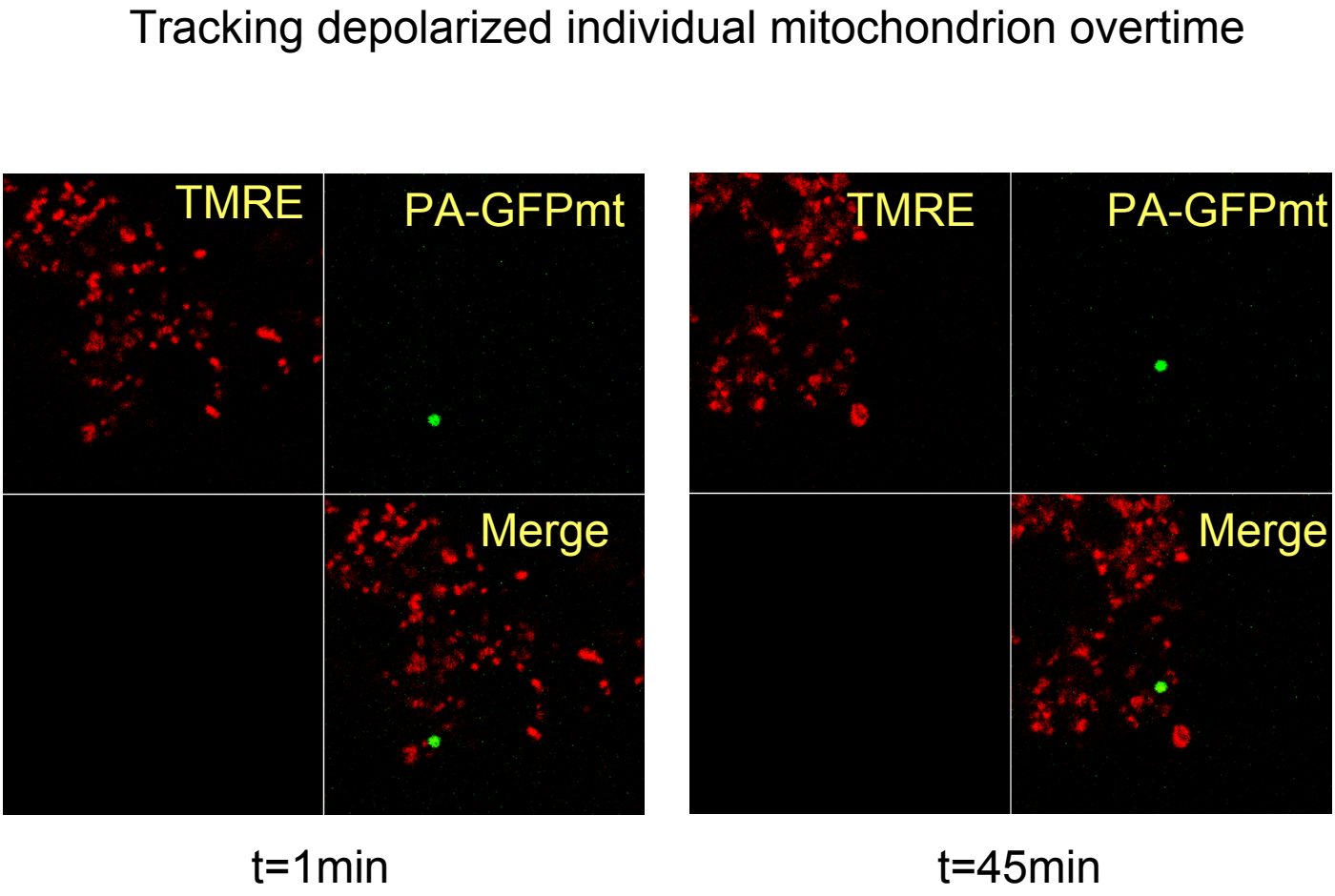

Figure S3: Tracking a depolarized mitochondrion over time. A single mitochondrion tagged with PA-GFP$_{mt}$ and tracked over time. This mitochondrion had reduced TMRE staining, and compared to average mitochondria in this cell, was 10-15 mV more positive. It was tracked for a period of 45 minutes. During that period this mitochondrion did not engage in a fusion or fission event and retained its' GFP FI during the recording period (GFP FI$_{(t=0)}$ = 233 ; GFP FI$_{(t=1\ hr)}$= 221). This experiment also shows that the depolarized level of the mitochondrion was independent of its location within cell, suggesting that limitations in diffusion of TMRE and oxygen concentration had little effect on $\Delta\psi_m$.

Figure S3

(a)

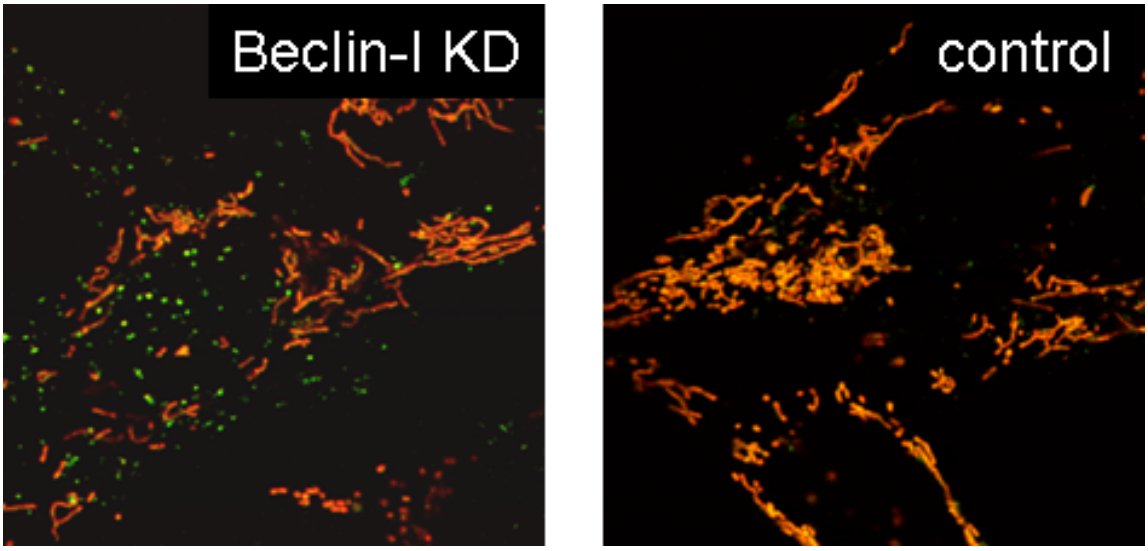

Merge images of TMRE (red) and Mitotracker Green (green)
Depolarized mitochondria appear in green

(b)

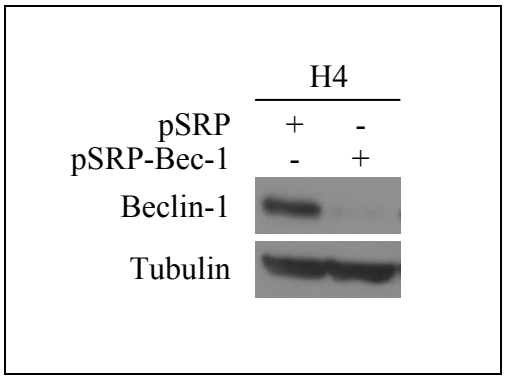

Figure S4: Inhibition of autophagy results in increased subcellular heterogeneity in mitochondrial membrane potential (a) **Knockdown of the autophagy protein, Beclin 1, in liver H4 cell line** results in the accumulation of small depolarized mitochondria. Depolarized mitochondria appear green. Mitotracker Green and TMRE (red). (b) Western blot analysis of Beclin 1 in shRNA treated cells and control.

Figure S4

(c)

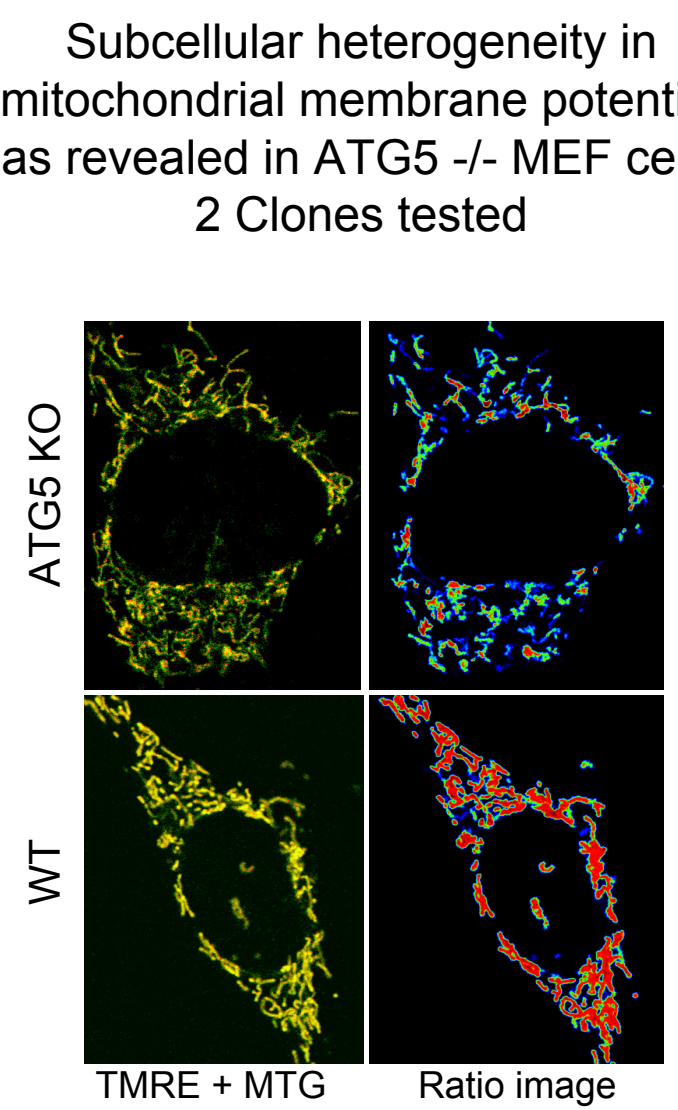

Figure S4 continued:
(c) ATG5 -/- MEF cells are characterized by depolarized mitochondria. Images are showing both merge of MTG and TMRE as well as a ratio image which is presented in FI coded color where blue color represents depolarized mitochondria.

Figure S4

(a)

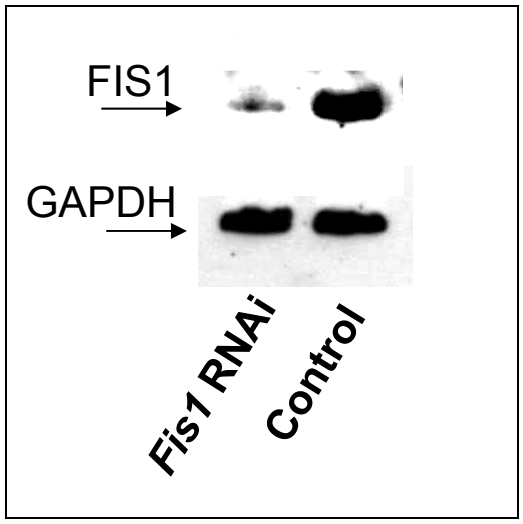

Knockdown of Fis1 using shRNA delivered by lentiviral transduction

(b)

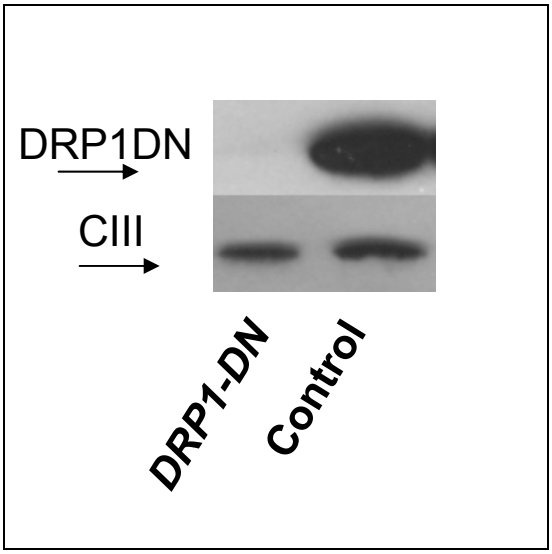

Expression of DRP1-DN delivered by lentiviral transduction

Figure S5: *Fis1* shRNA treatment and DRP1-DN expression. (a) INS1 cells were transduced with a vector carrying a previously described *Fis1* RNAi. After 2 weeks of cell culture, the level of FIS1 was measured using Western blot analysis. RT-PCR analysis demonstrated a reduction of *Fis1* mRNA levels by 87%± 7%. A single lentiviral infection (exposure of cells to virus for 4 hours) resulted in stable reduction of Fis1 transcript for 3 weeks. Reduction in gene expression was apparent 3 days after infection. (b) Expression of DRP1 dominant negative lentiviral transduction. DRP1-DN lentivirus had DRP1-DN clonedupstream of an IRES- EGFP sequence, which enabled the monitoring of the expression rate of the transgene. As a control cells were infected with the same virus expressing only GFP.

Figure S5

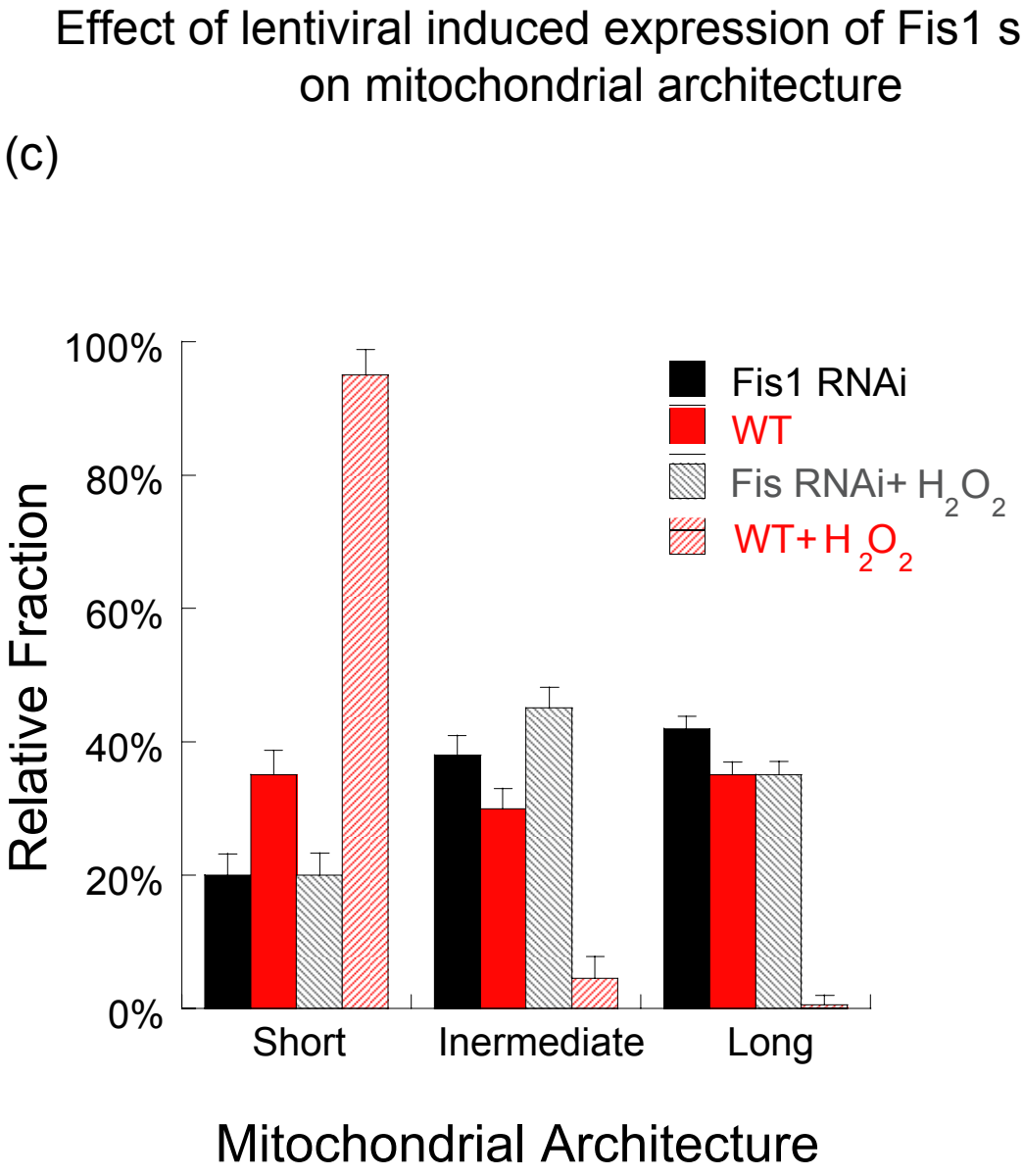

Figure S5 Continued:
(c) Morphometry analysis of mitochondria in cells infected with Fis1 KD lentivirus as compared to control shRNA virus. The geometric properties of mitochondrial webs were measured using the 'particle analysis' feature on ImageJ (NIH). A single web is defined as a continuous cluster of (at least 10) TMRE-positive pixels, regardless of matrix continuity. For each web, the perimeter, area maximal and minimal aspect length were measured and the aspect ratio (AR; maximal aspect divided by minimal aspect) was derived.

Figure S5

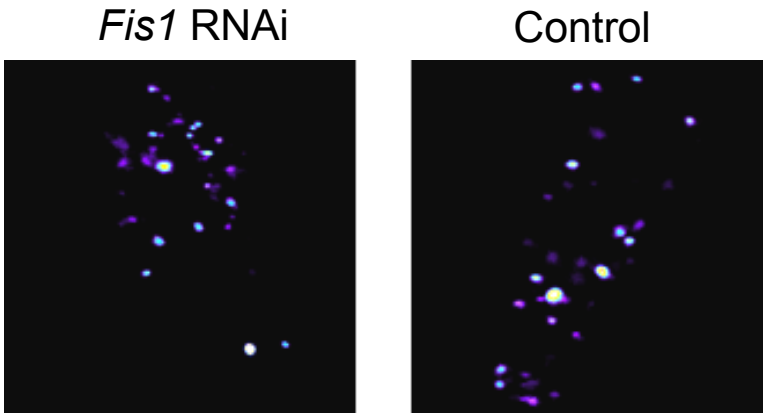

Lysosomes in INS1 cells

Figure S6: *Fis1* RNAi treatment does not reduce the total number of lysosomes. Lysosomes in INS1 cells were stained using lysosensor blue. Dye was loaded for 30 minutes and cells were imaged using 2-Photon confocal microscopy (Excitation/Emission 750/500-550 at 37C). Metamorph analysis was used to quantify the number of lysosomes based on fluoresce intensity and size (See Figure 6).

Figure S6

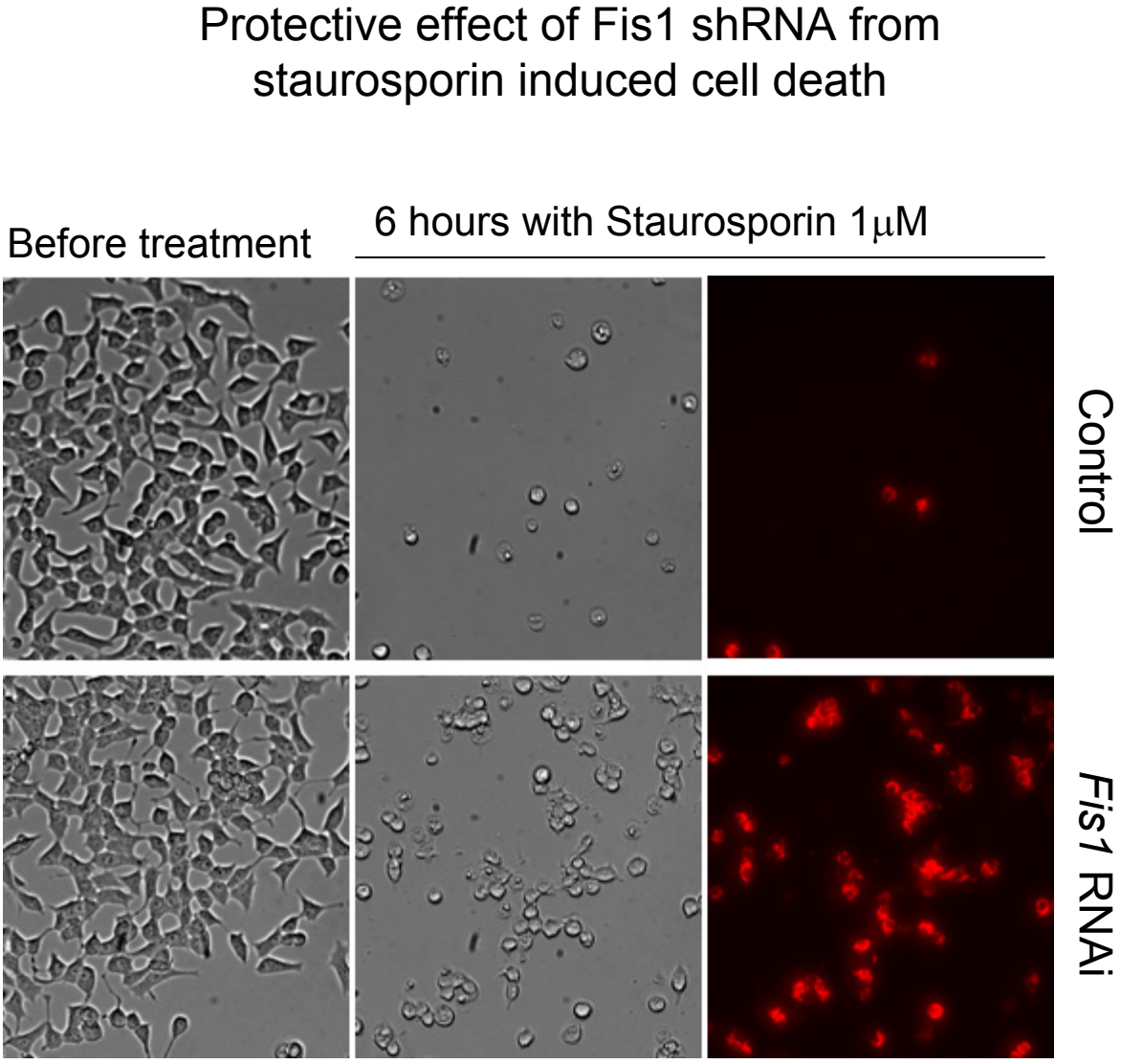

Figure S7: *Fis1* RNAi cells have increased resistance to apoptotic stimuli. INS1 cells expressing *Fis1* and control RNAi were stained with activated caspase 3 antibody following 6 hr treatment with staurosporine (1mM). Combined bright field and fluorescent images are shown. Red: activated caspase 3 positive cells are more abundant in control cells (left panel). This experiment supports the anti-apoptotic effect reported after *Fis1* silencing and indicates that the altered metabolic state seen in *Fis1* RNAi cells does not emerge from technical factors related to the RNAi construct or to the infection procedure

Figure S7

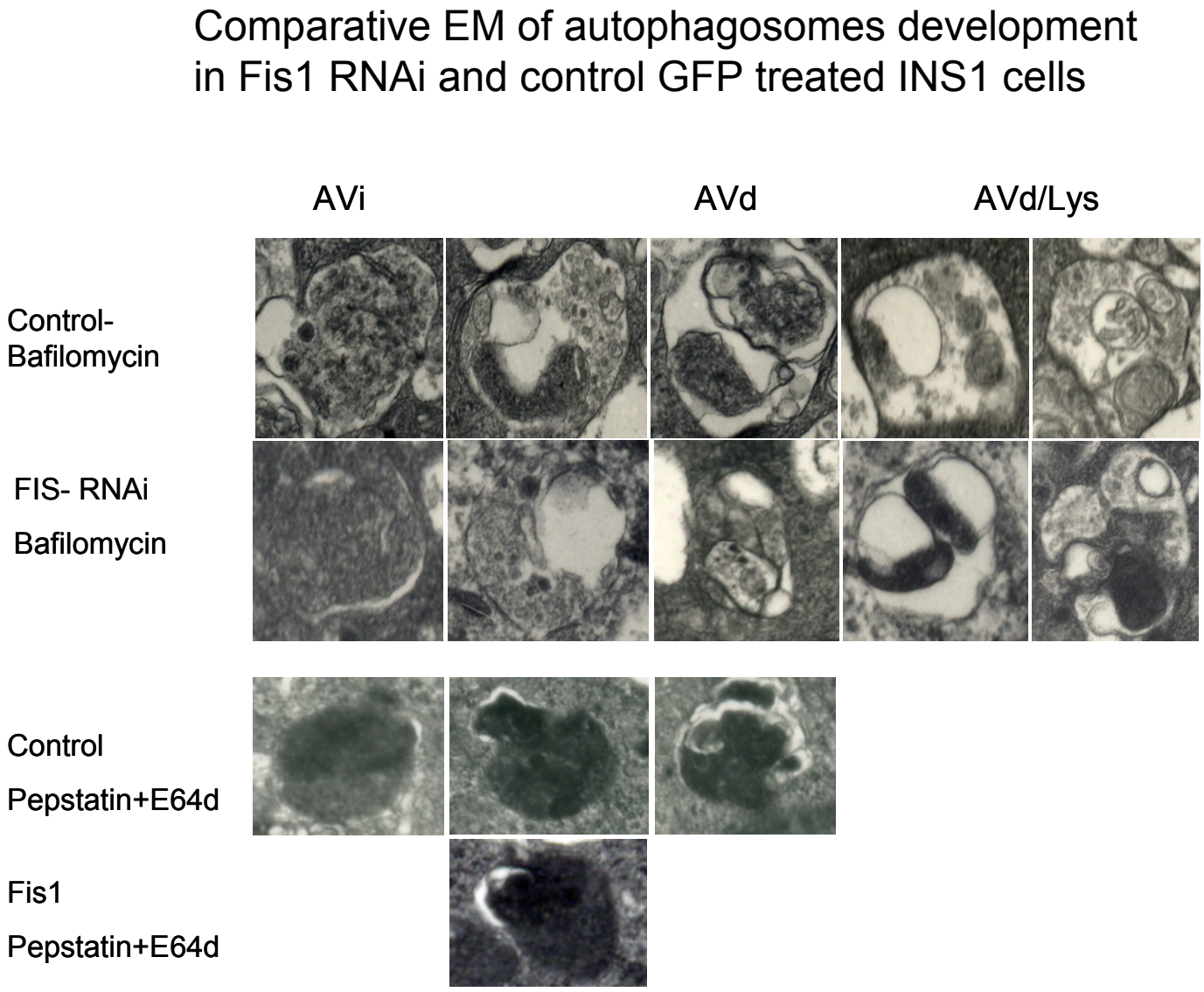

Figure S8: Electron Microscopic analysis of autophagosome maturation in Fis1KD and control. FIS KD and vector control INS-1 cells were treated with autophagosomes inhibitors Bafilomycin or Pepstatin+E64D, which block autophagy in early and late stages of autophagosome vacuole maturation respectively. Knocking Down of Fis-1 protein does not alter autophagosome maturation nor their morphology as revealed by the presence of AVi (Early/Initial autophagic vacuole), AVd (Late/Degradative autophagic vacuole) and AVd/Lys (Autolysosome)(Eskelinen, 2005).

Figure S8

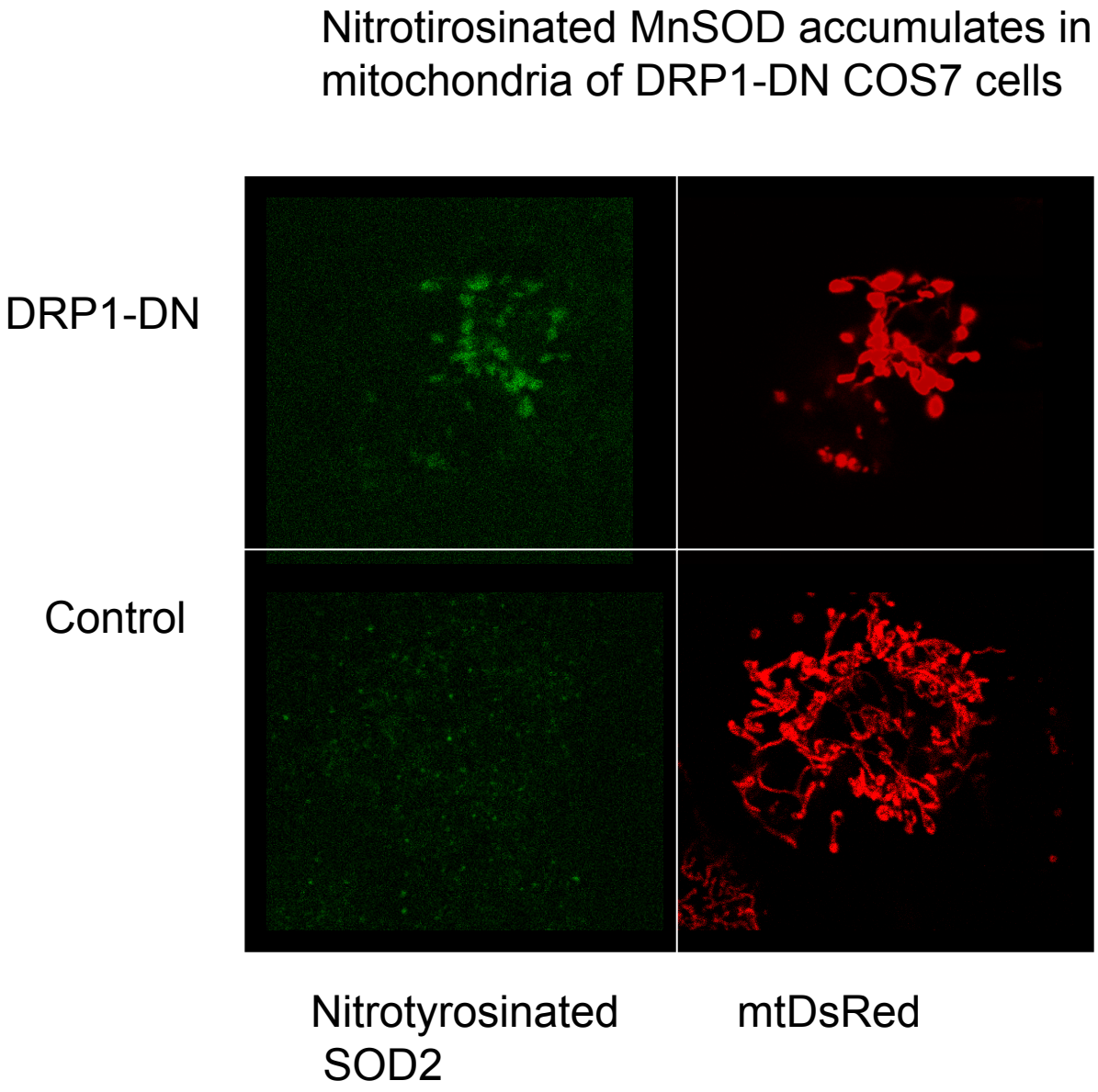

Figure S9: ***INS1 expressing DRP1-DN have increased level of oxidized MnSOD.***
COS7 cells co-expressing DRP1-DN and DsRed were stained with an antibody against the nitrotyrosinated form of MnSOD (SOD2) (Xu *et al.*, 2006). Control cells were infected with mtPAGFP lentivirus. One week post infection, cells were fixed, permeabilized and stained. Note that similar to the staining shown in figure 7, mitochondria in DRP1-DN accumulate oxidized protein in the thick, distal ending of each mitochondrion. Antibody is a gift of Dr. Richard Cohen, Boston University.

Figure S9

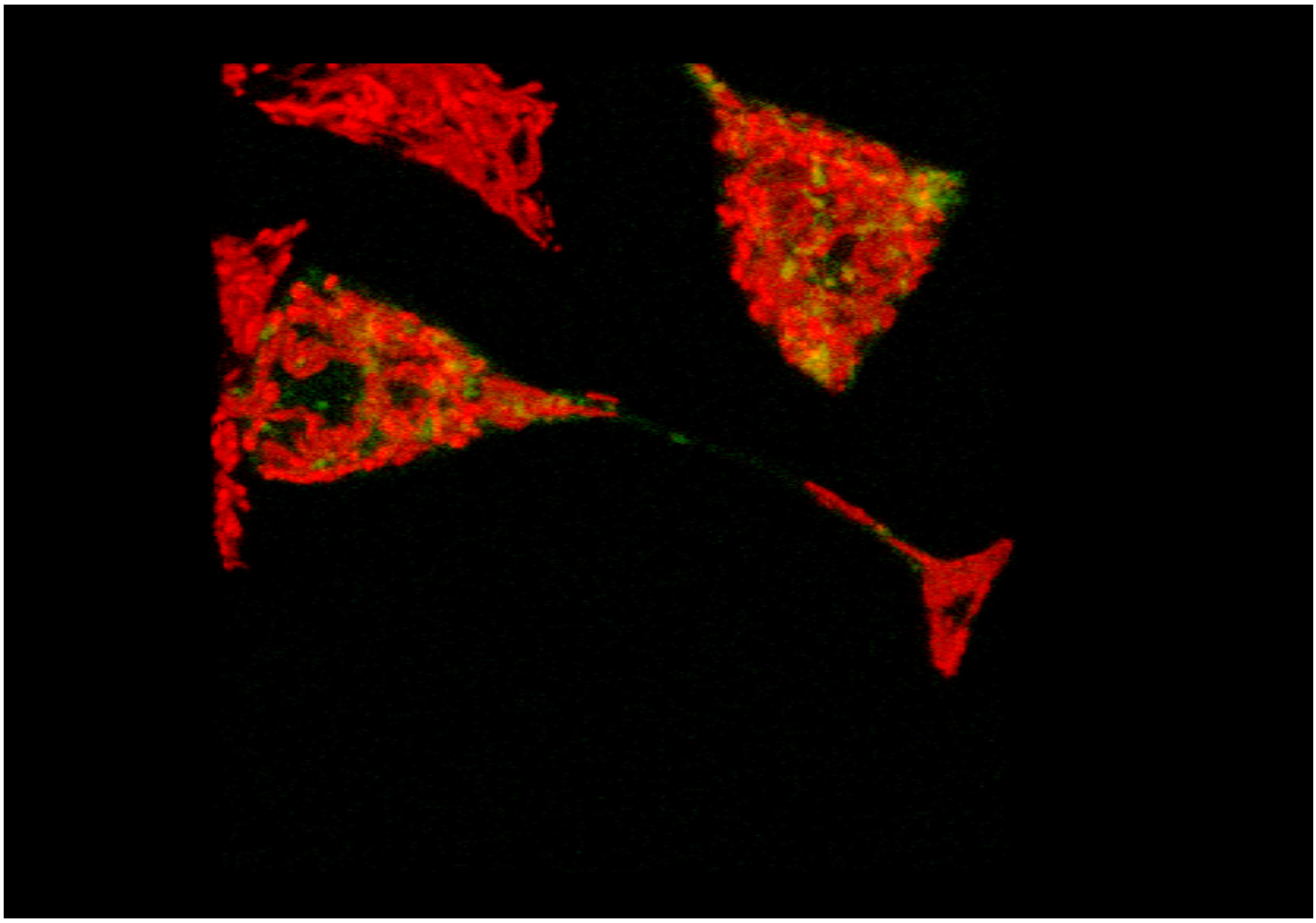

3D projection of 1Hr MTR Pulse experiment
Presented in figure 4

Green, LC3:GFP
Red, Mitotracker Red (MTR)

Figure S10: ***3D projection of INS1 cells expressing LC3GFP and stained with mitotracker red for the detection of mitochondrial autophagy as presented in Figure 4b.*** We used LC3:GFP, which translocates from the cytosol to the isolation membrane, to label early stages of AP assembly. Mitotracker red (MTR), a membrane potential dye that stains mitochondria irreversibly and is retained during depolarization, was used to pulse label mitochondria in INS1 cells (14 minutes, 50nM) at 1hour prior to detection of APs content. For detection cells were treated with pepstatin A (10mM) and E64d (10mM) for 30 minutes to arrest digestion inside the APs, then subjected to confocal microscopy (see schematic illustration of experiment protocol at Fig. 4b). While mitochondria outside APs showed bright MTR fluorescence, those localized in APs had reduced MTR, indicating that at the time of MTR pulse they were already depolarized.

Figure S10